

Defect evolution and interplay in n-type InN

Christian Rauch,^{1,*} Filip Tuomisto,¹ Arantxa Vilalta-Clemente,² Bertrand Lacroix,²
Pierre Ruterana,² Simon Krausel,³ Ben Hourahine,³ and William J. Schaff⁴

¹Department of Applied Physics, Aalto University,
P.O. Box 11100, FI-00076 Aalto, Espoo, Finland

²CIMAP UMR 6252 CNRS-ENSICAEN-CEA-UCBN, 6,
Boulevard du Maréchal Juin, 14050 Caen Cedex, France

³Department of Physics, SUPA, Strathclyde University, G4 0NG Glasgow, United Kingdom

⁴Department of Electrical and Computer Engineering,
Cornell University, 425 Philips Hall, Ithaca, New York 14853, USA

(Dated: November 6, 2018)

The nature and interplay of intrinsic point and extended defects in n-type Si-doped InN epilayers with free carrier concentrations up to $6.6 \times 10^{20} \text{cm}^{-3}$ are studied using positron annihilation spectroscopy and transmission electron microscopy and compared to results from undoped irradiated films. In as-grown Si-doped samples, $V_{\text{In}}-V_{\text{N}}$ complexes are the dominant III-sublattice related vacancy defects. Enhanced formation of larger $V_{\text{In}}-mV_{\text{N}}$ clusters is observed at the interface, which speaks for a high concentration of additional V_{N} in the near-interface region and coincides with an increase of the dislocation density in that area.

InN possesses a strong propensity for n-type conductivity which can be explained by an exceptionally high Fermi stabilization energy [1] well above the conduction band minimum. Taming the conductivity is one requirement for exploiting the material's high potential for electronic and opto-electronic devices [2]. Therefore, a deep understanding of the defect landscape in n-type InN is required. *Ab-initio* calculations predict that hydrogen acts as an effective donor impurity in InN [3], while V_{N} and V_{In} should be the dominant intrinsic donor and acceptor type point defects [4]. Additionally, high densities of extended defects are commonly found in as-grown material and have been correlated with an electron accumulation layer at InN interfaces [5]. In this letter, we use positron annihilation spectroscopy (PAS) and transmission electron microscopy (TEM) to study the evolution and interplay of native point and extended defects in highly n-type InN under different conditions. Si-doped InN layers [7] with free electron concentrations from 4.5×10^{19} - $6.6 \times 10^{20} \text{cm}^{-3}$ are investigated and compared to results from an undoped ($n_e = 1 \times 10^{18} \text{cm}^{-3}$ before irr.) irradiated InN film [6] before ($3.2 \times 10^{20} \text{cm}^{-3}$) and after annealing ($6 \times 10^{19} \text{cm}^{-3}$). All films were deposited by plasma-assisted molecular beam epitaxy (PAMBE) as $\sim 500 \text{nm}$ thick layers on c-plane sapphire substrates with a GaN buffer layer [6, 7].

TEM measurements of thin cross-sectional samples were performed using a JEOL 2010 operating at an acceleration voltage of 200 kV [8]. Fig. 1 shows a TEM micrograph obtained in weak beam (WB) conditions with $g=11\bar{2}0$ for a representative Si-doped sample. Edge and mixed type dislocations are visible distributed throughout the InN layer with an average density of $4.0 \times 10^9 \text{cm}^{-2}$ and $1.1 \times 10^9 \text{cm}^{-2}$, respectively.

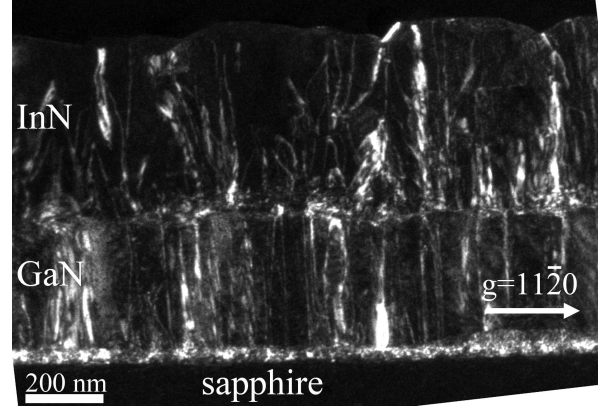


FIG. 1: Cross-sectional dark-field TEM micrograph ($g=11\bar{2}0$) of a representative Si-doped sample ($n_e=4.0 \times 10^{20} \text{cm}^{-3}$), showing edge and mixed type dislocations.

An agglomeration of dislocations close to the InN/GaN interface can be noticed. The density of screw type dislocations is $3.1 \times 10^8 \text{cm}^{-2}$ which corresponds to $\sim 6\%$ of the total dislocation density. Additionally, a high density ($3 \times 10^5 \text{cm}^{-1}$) of stacking faults was revealed for WB conditions [8] with $g=10\bar{1}0$ (not shown here). In the irradiated InN film, earlier TEM results [9] showed irradiation-induced formation dislocation loops in addition to a significant density of planar defects introduced during growth. After annealing at 475°C the density of dislocation loops increased from $2.2 \times 10^{10} \text{cm}^{-2}$ to $9.0 \times 10^{10} \text{cm}^{-2}$ [6, 9]. Vacancy agglomeration after annealing was proposed as reason for this increase. We applied PAS to investigate vacancy-type point defects and their nature in the InN samples. Using a mono-energetic positron beam, depth-dependent Doppler broadening spectra were recorded at room temperature to probe the momentum distribution of annihilating electron-positron pairs. Details on the experimental tech-

*Electronic address: christian.rauch@aalto.fi

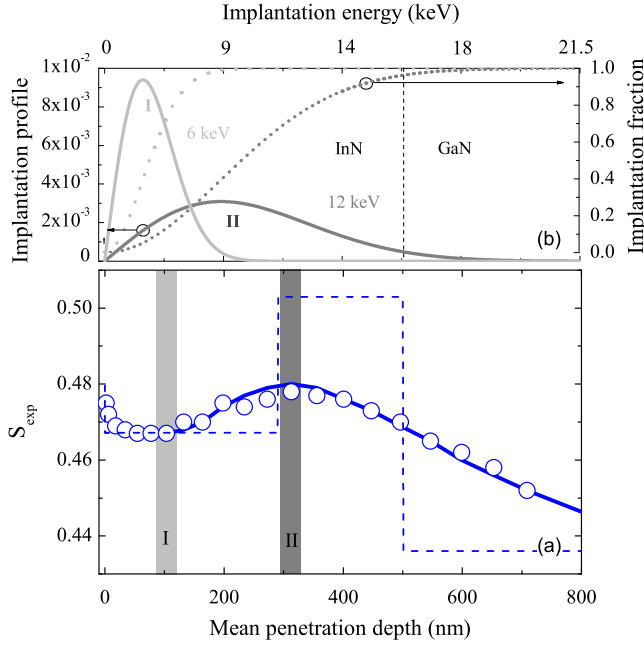


FIG. 2: (Color online) Measured S parameter (open circles) of sample 2 as function of the mean positron implantation depth (a). Corresponding implantation energies are given for comparison. The solid line shows a fit of the data using a simple three-layer model of the S-parameter (dashed line). Fig. (b) shows the calculated positron implantation profiles and fractions for positron implantation energies of 6 keV (I) and 12 keV (II).

nique and setup can be found elsewhere [10, 11]. Fig. 2(a) shows the measured S-parameters of a representative Si-doped sample for positron implantation energies from 0-20 keV. After annihilation at surface-specific states for low implantation energies, the S-parameter drops quickly to a local minimum at ~ 6 keV. Comparison with the positron implantation profile at that energy [Fig. 2(b)] reveals that this point is representative for annihilations from the first 150 nm of the sample, with a mean implantation depth of $\bar{x}=100$ nm. Deeper inside the sample, the S-parameter increases to a local maximum at ~ 12 keV (corresponding to a mean implantation depth of $\bar{x}=310$ nm) and positrons probe a wide region reaching the interface to the GaN buffer layer. For higher implantation energies a significant amount of positrons annihilate in the GaN buffer layer pulling the measured S-parameter towards the value of the GaN lattice. The solid curve in Fig. 2(a) shows a fit of the measured spectrum using the multi-layer fitting program VEP-FIT [12]. It reveals that the experimental spectrum can be well described assuming a two-layer structure of the S-parameter inside the InN film (see dashed line) with a 300 nm thick near-surface and 200 nm thick near-interface layer and a positron diffusion length of ~ 5 nm.

Representative for the near-surface ("layer") and near-interface ("interface") areas, the measured S and W parameter at 6 and 12 keV are plotted in Fig. 3 together with accordingly determined values of the remaining

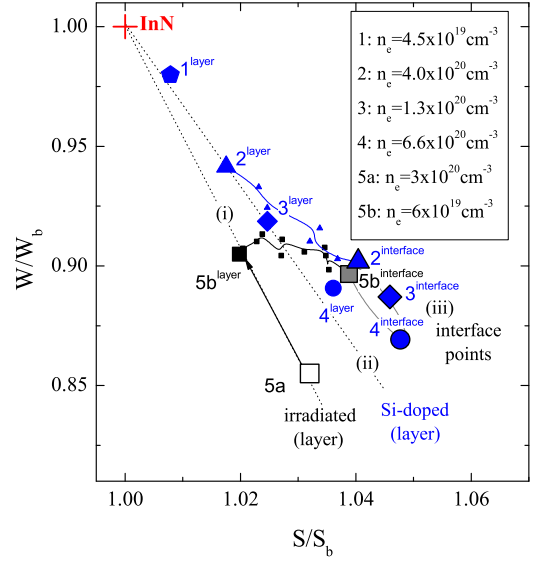


FIG. 3: (Color online) S and W line-shape parameters of the Doppler broadened electron-positron annihilation γ -radiation for different samples and areas.

samples. All points are normalized by the value of an InN reference sample for which no positron trapping at open volume defects is observed [11]. Samples 1 and 5a did not exhibit any depth-profile and therefore only one set of parameters is displayed. For all Si-doped samples (samples 1-4), the "layer" points fall on one line through the reference value of the InN lattice. Hence [10], one dominant vacancy-type positron trap is present in this area with increasing (room-temperature) annihilation fraction from sample 1-4. For the "interface" points, a deviation from the "layer" line is visible due to increasing S-parameters and comparably less pronounced decrease in the W-parameters. Therefore, a different dominant vacancy-type positron trap has to be expected here. The slope defined by the irradiated sample before annealing (sample 5a) is steeper [13] than for the as-grown samples. Upon rapid thermal annealing (RTA) [6] (sample 5b), a profile in the depth dependent spectrum of the S-parameter is developed [14] with a layer and interface-specific value. The near-surface "layer"-point is shifted closer toward the InN lattice point but remains on the same line as the as-irradiated sample. This indicates a decrease in annihilation fraction at the same positron trap as before annealing. The "interface" point, however, deviates strongly after annealing and is moved close to the interface points of the Si-doped samples.

We find 3 different dominant vacancy-type positron traps in the InN samples, i.e., defects created by high-energy particle irradiation (i), defects dominant at the near-surface area of as-grown Si-doped samples (ii), and defects responsible for the observed changes at the interfaces of both Si-doped as well as RTA-treated, irradiated samples (iii). A comparison of high-resolution coincidence Doppler broadening spectra with density func-

tional theory (DFT) calculations of positron trapping and annihilation in InN reveals [11] that these positron traps can be identified as (i) isolated In vacancies (V_{In}), (ii) mixed In-N divacancies ($V_{\text{In}}-V_{\text{N}}$), and (iii) bigger $V_{\text{In}}-mV_{\text{N}}$ ($m \approx 2, 3$) vacancy complexes, respectively. High-energy particle irradiation introduces isolated V_{In} as dominant vacancy-type positron traps in InN. Subsequent annealing leads to a re-arrangement of vacancy defects [14], as observable in both TEM and positron annihilation measurements. V_{In} become mobile at or below the annealing temperature and start to move toward the surface and the interface with the GaN buffer, respectively, where they either recombine, anneal out (at the surface) or form complexes with residual V_{N} (interface). Based on the employed annealing temperature of 475°C, we can estimate [15] an upper limit of $E_b \leq 1.9$ eV for the migration barrier of the V_{In} . This is in good agreement with the calculated value of 1.6 eV [16] and indicates that isolated V_{In} are mobile during InN growth (assuming usual growth temperatures of $\sim 550^\circ\text{C}$ for, e.g., MBE). No isolated V_{In} are observed in our measurements of as-grown Si-doped InN. Instead, we find $V_{\text{In}}-V_{\text{N}}$ complexes. Hence, we conclude that in-grown V_{In} are stabilized through the formation of complexes with V_{N} . This is supported by recent DFT results [16] which predict a positive binding energy between V_{In} and V_{N} . Vacancy-stabilization through the formation of vacancy-donor complexes has been observed also in GaN (Ref. [17], and references therein) and AlN [18]. The increased incorporation of V_{In} complexes with increasing free electron concentration suggests strongly that V_{In} -related defects act as a source of compensation in n-type InN, which is in line with theoretical results [4]. The enhanced formation of larger $V_{\text{In}}-mV_{\text{N}}$ complexes toward the interface with the GaN buffer layer (in irradiated material after annealing as well as Si-doped samples) indicates that the InN/GaN interface is attractive for vacancy defects. An additional high density of V_{N} in that area could provide the proximity required for the promotion of efficient vacancy $V_{\text{In}}-mV_{\text{N}}$ clustering. However, neutral and positively charged isolated V_{N} and mV_{N} -complexes can not be detected in PAS measurements [11]. Duan *et al.* have calculated [19] a positive binding energy between single V_{N} under n-type conditions and a strong tendency for the formation of larger V_{N} clusters. Hence, the formation of $V_{\text{In}}-mV_{\text{N}}$ complexes could occur through a precursor state of $mV_{\text{N}} + V_{\text{In}} \rightarrow V_{\text{In}}-mV_{\text{N}}$, in accordance to what has been proposed earlier in Mg-doped InN [20].

Based on the TEM data, the observed increase in vacancy clustering at the InN/GaN interface coincides with elevated dislocation densities in that area. In order to assess the effect of dislocations on the formation energies of point defects in their vicinity we performed DFT calculations of strained InN lattices. We found that typical strain associated with screw dislocations (0-15% shear) decreases the formation energies of V_{In} and V_{N} only slightly by ≤ 30 meV, and hence should not play any major role. Investigations on the effects of edge dislocations are under way. Besides strain-related influences on the defect formation energies, additional dislocation-related vacancy formation mechanisms such as dislocation movement and/or decoration of dislocations might be possible. In GaN, recent theoretical calculations [21] suggest stable configurations of vacancies inside dislocation cores and a correlation between vacancy densities and dislocations was found [22]. It should be noted that dislocations might also directly affect the positron annihilation signal [23] by, e.g., forming shallow traps for positrons. The exceptionally low values of the positron diffusion length in the InN samples do support the presence of such additional positron trapping centers with annihilation characteristics close to the bulk. Detailed theoretical investigations on positron trapping and annihilation at dislocations in wurtzite semiconductors are currently being performed.

In summary, combining results from PAS and TEM we find that isolated V_{In} are only present in irradiated InN films and anneal out at temperatures of $\leq 475^\circ\text{C}$ if not stabilized by other point defects. Stabilization of V_{In} occurs through complex formation with V_{N} . $V_{\text{In}}-mV_{\text{N}}$ complexes are the dominant vacancy-type positron trap in as-grown InN samples. Toward the interface between the InN layer and the GaN buffer, enhanced formation of bigger vacancy clusters with increasing number of V_{N} is observed in both as-grown and irradiated material after annealing and coincides with increased dislocation densities in that area. This indicates that the InN/GaN interface is strongly attractive for vacancy defects and points at elevated concentrations of additional V_{N} and V_{N} -complexes in that area.

The authors wish to thank T. Veal for helpful discussions. This work has been supported by the European Commission under the 7th Framework Program through the Marie Curie Initial Training Network RAINBOW, Contract No. PITN-Ga-2008-213238, and the Academy of Finland.

-
- [1] P. D. C. King, T. D. Veal, P. H. Jefferson, S. A. Hatfield, L. F. J. Piper, C. F. McConville, F. Fuchs, J. Furthmüller, F. Bechstedt, H. Lu, et al., Phys. Rev. B **77**, 045316 (2008).
 - [2] B. Monemar, J. Mater. Sci. Mater. Electron. **10**, 227 (1999).
 - [3] A. Janotti and C. G. Van de Walle, **92**, 032104 (2008).

- [4] C. Stampfl, C. G. Van de Walle, D. Vogel, P. Krüger, and J. Pollmann, Phys. Rev. B **61**, R7846 (2000).
- [5] L. F. J. Piper, T. D. Veal, C. F. McConville, H. Lu, and W. J. Schaff, Appl. Phys. Lett. **88**, 252109 (2006).
- [6] R. E. Jones, S. X. Li, E. E. Haller, H. C. M. van Genuchten, K. M. Yu, J. W. Ager III, Z. Liliental-Weber, W. Walukiewicz, H. Lu, et al., Appl. Phys. Lett. **90**,

- 162103 (2007).
- [7] W. J. Schaff, H. Lu, L. F. Eastman, W. Walukiewicz, K. M. Yu, S. Keller, S. Kurtz, B. Keyes, and L. Gevilas, in *State-of-the-Art Program on Compound Semiconductors XLI and Nitride and Wide Bandgap Semiconductors for Sensors, Photonics, and Electronics V*, edited by H. M. Ng and A. G. Baca (Electrochemical Society, Honolulu, HI, 2004), vol. 2004-06 of *The Electrochemical Society Proceedings Series*, p. 358.
 - [8] Y. Arroyo Rojas Dasilva, M. P. Chauvat, P. Ruterana, L. Lahourcade, E. Monroy, and G. Nataf, *J. Phys. Cond. Matt.* **22**, 355802 (2010).
 - [9] Z. Liliental-Weber, R. Jones, H. van Genuchten, K. Yu, W. Walukiewicz, J. W. Ager III, E. Haller, H. Lu, and W. Schaff, *Physica B* **401-402**, 646 (2007).
 - [10] K. Saarinen, P. Hautojärvi, and C. Corbel, *Positron Annihilation Spectroscopy of Defects in Semiconductors*, vol. 51A of *Semiconductors and Semimetals* (Academic Press, New York, 1998).
 - [11] C. Rauch, I. Makkonen, and F. Tuomisto, *Phys. Rev. B* **84**, 125201 (2011).
 - [12] A. van Veen, H. Schut, M. Clement, J. M. M. de Nijs, A. Kruseman, and M. R. IJpma, *Appl. Surf. Sci.* **85**, 216 (1995).
 - [13] F. Tuomisto, A. Pelli, K. M. Yu, W. Walukiewicz, and W. J. Schaff, *Phys. Rev. B* **75**, 193201 (2007).
 - [14] F. Reurings, C. Rauch, F. Tuomisto, R. E. Jones, K. M. Yu, W. Walukiewicz, and W. J. Schaff, *Phys. Rev. B* **82**, 153202 (2010).
 - [15] S. Limpijumnong and C. G. Van de Walle, *Phys. Rev. B* **69**, 035207 (2004).
 - [16] X. M. Duan and C. Stampfl, *Phys. Rev. B* **79**, 174202 (2009).
 - [17] F. Tuomisto, T. Paskova, R. Kroger, S. Figge, D. Hommel, B. Monemar, and R. Kersting, *Appl. Phys. Lett.* **90**, 121915 (2007).
 - [18] J.-M. Mäki, I. Makkonen, F. Tuomisto, A. Karjalainen, S. Suihkonen, J. Räisänen, T. Y. Chemekova, and Y. N. Makarov, *Phys. Rev. B* **84**, 081204 (2011).
 - [19] X. M. Duan and C. Stampfl, *Phys. Rev. B* **77**, 115207 (2008).
 - [20] A. Uedono, H. Nakamori, K. Narita, J. Suzuki, X. Wang, S. B. Che, Y. Ishitani, A. Yoshikawa, and S. Ishibashi, *J. Appl. Phys.* **105**, 054507 (2009).
 - [21] S. Krausel and B. Hourahine *Phys. Status Solidi A* DOI:10.1002/pssa.201100097 (2011).
 - [22] J. Oila, J. Kivioja, V. Ranki, K. Saarinen, D. C. Look, R. J. Molnar, S. S. Park, S. K. Lee, and J. Y. Han, *Appl. Phys. Lett.* **82**, 3433 (2003).
 - [23] E. Tengborn, M. Rummukainen, F. Tuomisto, K. Saarinen, M. Rudzinski, P. R. Hageman, P. K. Larsen, and A. Nordlund, *Appl. Phys. Lett.* **89**, 091905 (2006).